http://doi.org/10.35784/iapgos.7788 received: 20.05.2025 | revised: 27.12.2025 | accepted: 02.06.2026 | available online: 30.06.2026

METHOD OF STRUCTURAL-BLOCK CODING OF TUPLE TRANSFORMANT VIDEO IMAGES

Volodymyr Barannik[1], Dmytro Uzlov[1], Yevhenii Yelisieiev[2], Valeriy Barannik[1], Nina Petrukha[3], Mykhailo Babenko[2], Dmitry Barannik[4], Vladyslav Kostromytskyi[2], Oleh Kompaniiets[5], Artem Bychenko[6]

[1]V.N. Karazin Kharkiv National University, Kharkiv, Ukraine, [2]Kharkiv National University of Radio Electronics, Kharkiv, Ukraine, [3]Kyiv National University of Construction and Architecture, Kyiv, Ukraine, [4]Heroes of Kruty Military Institute of Telecommunications and Informatization, Kyiv, Ukraine, [5]Ivan Kozhedub Kharkiv National Air Force University, Kharkiv, Ukraine, [6]National University of Civil Defense, Cherkasy, Ukraine

Abstract. *In the modern world, the quality of video information services is important. The greatest difficulties arise in the case of providing remote services using wireless information and communication systems (ICS). This concerns the imbalance between the intensity of the video stream and the speed of data transmission in the ICS. Elimination of the imbalance is possible using compression methods. However, compression of the bit volume of video data is achieved with a loss of integrity. Hence, a relevant scientific and applied problem is the further improvement of coding methods based on the elimination of various types of redundancy. At the same time, most methods are characterized by achieving the desired level of compression by introducing distortions. This necessitates the development of a compression direction based on the controlled elimination of the number of different types of redundancy. Accordingly, to create conditions for increasing the possibilities for detecting characteristic dependencies, the technological apparatus of converting video segments to spectral space is used. Therefore, the research goal of the article is to develop compression methods based on a controlled reduction in the number of different types of redundancy in spectral space. The article outlines the main stages of developing a method for structural block coding of transform tuples. To increase the compression level without loss of integrity, it is proposed to identify characteristic structural dependencies for a set of transforms. Such sets are divided into tuples according to the parametric data of the structural and spectral features of the transforms. Further, such a space will be referred to as the spectral and parametric description of transforms (SPDT). Comparative evaluation of compression methods is carried out according to the system of indicators: compression level - integrity level. Under such conditions, the advantage of the created method over basic analogues in terms of compression level is from 12 to 19%.*

Keywords: video data, information systems, compression, clustering, video segment transform, structural block coding, redundancy

METODA STRUKTURALNEGO KODOWANIA BLOKOWEGO KROTEK TRANSFORMACJI OBRAZÓW WIDEO

Streszczenie. *We współczesnym świecie jakość usług związanych z przekazem obrazu ma duże znaczenie. Największe trudności pojawiają się w przypadku świadczenia usług zdalnych z wykorzystaniem bezprzewodowych systemów informacyjno-komunikacyjnych (ICS). Dotyczy to nierównowagi między intensywnością strumienia wideo a prędkością transmisji danych w ICS. Wyeliminowanie tej nierównowagi jest możliwe dzięki zastosowaniu metod kompresji. Jednak kompresja objętości bitowej danych wideo wiąże się z utratą integralności. Stąd też istotnym problemem naukowym i praktycznym jest dalsze udoskonalanie metod kodowania opartych na eliminacji różnych rodzajów nadmiarowości. Jednocześnie większość metod charakteryzuje się osiąganiem pożądanego poziomu kompresji poprzez wprowadzanie zniekształceń. Wymaga to opracowania kierunku kompresji opartego na kontrolowanej eliminacji różnych rodzajów nadmiarowości. W związku z tym, aby stworzyć warunki do zwiększenia możliwości wykrywania charakterystycznych zależności, wykorzystuje się aparaturę technologiczną przekształcającą segmenty wideo do przestrzeni spektralnej. W związku z tym celem badawczym niniejszego artykułu jest opracowanie metod kompresji opartych na kontrolowanym zmniejszeniu liczby różnych rodzajów nadmiarowości w przestrzeni spektralnej. W artykule nakreślono główne etapy opracowywania metody strukturalnego kodowania blokowego krotek transformacji. Aby zwiększyć stopień kompresji bez utraty integralności, proponuje się zidentyfikowanie charakterystycznych zależności strukturalnych dla zbioru transformacji. Zbiory takie dzieli się na krotki zgodnie z danymi parametrycznymi cech strukturalnych i spektralnych transformacji. Ponadto taka przestrzeń będzie określana jako spektralny i parametryczny opis transformacji (SPOT). Ocena porównawcza metod kompresji przeprowadzana jest zgodnie z systemem wskaźników: poziom kompresji – poziom integralności. W takich warunkach przewaga opracowanej metody nad podstawowymi odpowiednikami pod względem poziomu kompresji wynosi od 12 do 19%.*

Słowa kluczowe: dane wideo, systemy informacyjne, kompresja, klasteryzacja, przekształcanie segmentów wideo, strukturalne kodowanie blokowe, redundancja

Introduction

Modern services providing various informational functionalities are closely tied to the generation of large volumes of traffic that must be transmitted through telecommunication networks [1]. A significant portion of this traffic is comprised of video data streams. Notable examples include applications in critical infrastructure management, and the analysis of information flows in large-scale projects like "Smart City" and "Safe City." Consequently, certain qualitative requirements are imposed on such information, including timeliness of delivery, accuracy, visual quality, and structural integrity of monitored objects [3]. This drives the growing demand for technologies that reduce the volume of informational traffic, primarily through the implementation of data compression methods in information processing systems [4].

Over the years, a vast array of methodological approaches to video data compression has been developed [2, 5], including multiple families and improved versions of standardized methods [6, 10]. These methods have significantly reduced traffic intensity, easing the load on telecommunication networks and enabling control centers to receive timely information as required [7]. However, user demands for information services continue to grow. Increasing reliance on video data from remote sensors [16, 17] has highlighted significant delays in data transmission. These delays arise from a fundamental conflict between the timeliness of video information delivery and its accuracy, including the visual quality of reconstructed video images [8]. Thus, advancing video data compression methods to mitigate this conflict has become a ***critical scientific and practical challenge***.

Generally, two classes of comprehensive methods are employed to address this issue [9, 11]:

1) lossless compression methods. These preserve the integrity of the information but typically achieve insufficient levels of compression [12, 26];
2) loss compression methods. These introduce quality distortions in video images, such as JPEG and Web standards [14, 20]. These methods are more popular due to their higher compression efficiency [13 ,15].

The ongoing enhancement of video data compression technologies is influenced by several factors [18, 19]:

- increasing image format sizes;
- utilization of images for situational analysis during crises;
- addressing resource conflicts related to networks, clouds, and computational capacities [21];
- development of artificial intelligence systems and their integration into automated management systems [22];
- the growing user base of modern multimedia services.

This evolution underscores the demand for improved qualitative parameters in compression methods, particularly

This work is licensed under a Creative Commons Attribution 4.0 International License.
Utwór dostępny jest na licencji Creative Commons Uznanie autorstwa 4.0 Międzynarodowe.

in terms of compression efficiency and distortion levels in digitized video images (e.g., measured by the Peak Signal-to-Noise Ratio, PSNR) [24, 25]. However, these metrics often exhibit inverse relationships [27, 29], where higher compression ratios result in reduced image quality [28].

The necessity to address these contradictions has led to the development of various classes of image compression methods [30]. The most integrated solutions in modern information technologies are those based on comprehensive processing techniques. These approaches include stages such as pre-processing, redundancy elimination, post processing, and enhancement of visual quality [23]. However, existing compression methods exhibit several notable drawbacks [23]:

- achieving target compression levels often comes at the expense of image quality, resulting in artefacts, distortions in contour information, and degradation of fine details;
- a disproportionate relationship exists between the significant added complexity of algorithmic implementation and the limited additional reduction in redundancy achieved;
- additional compression gains are often accompanied by the generation of considerable auxiliary metadata, which decreases the overall efficiency of image compression.

To overcome these limitations, this study proposes focusing on compression methods that operate under a regime of controlled quality distortions. One promising direction involves pre-processing image fragments in the spectral domain. Therefore, the ***objective of this research*** is to develop compression methods with controlled quality distortions by leveraging pre-processing in the spectral domain.

1. Analysis of current research and problem statement

To eliminate this imbalance, it is necessary to create technologies for reducing the bit volume of video data [8, 16]. However, modern technologies have a significant drawback. It concerns the dependence of the bit compression level of video images on the amount of psych visual redundancy in it [9, 11, 12, 26].

Accordingly, for the vast majority of realistic video images, this amount is limited. This leads to one of two possible events [13–15, 18, 20]:

- in the case of a static model, the elimination of the amount of psych visual redundancy leads to the loss of integrity of video images or their partial destruction;
- in the case of a variable model, reducing the amount of psych visual redundancy leads to a significant reduction in the compression level. This increases the time delay for information delivery.
- To eliminate such shortcomings, it is necessary to develop new technologies for video data compression coding [19, 21].

Therefore, the **scientific and applied problem** of creating new compression coding technologies in the context of localising the balance between the efficiency of video data delivery and its integrity is relevant.

2. Justification for improving compression methods with controlled image quality

The specific enrichment of a standardized processing pipeline with technological tools is determined by the characteristics of applied tasks. In scenarios where applications are tied to real-time requirements, such as live streaming and/or exchange of "live" video, the following factors become prominent:

1) primary metric: The interval of transmission delays for video delivery;
2) secondary metric: The quality of video on the recipient's (end-user's) side.

These criteria impose technological constraints on the implementation of the compression pipeline. In this context, pre-processing that involves the formation of a spectral-parametric (SPDT) description of the transformant can be employed.

A spectral–parametric description of a transformant (SPDT) [4] is defined as a representation in which the transformant $Y(t;\delta)$ is modelled as a two-parameter set of spectral sub-bands $sb(t;\delta)_{\alpha}$, parameterized by $L(t;\delta)$ and $S(t;\delta)$.

A spectral sub-band (SSBP) is a sequence of transformant components $y(\delta)_{t,\alpha,\gamma}$ obtained by diagonal scanning, whose values can be approximated by a zero- or first-order spline while maintaining the required level of information integrity. In other words, a sub-band is a sequence of spectral components with only minor variations in their values. This property allows the component values within a sub-band to be approximated by an average value $sb(t;\delta)_{\alpha}$. Accordingly, the SSBP length $\ell(\delta)_{t,\alpha}$ is determined by the number of components that satisfy these conditions.

This approach allows for adjustments based on two critical parameters: compression level and computational load. To achieve these adjustments, the range of intervals for constructing spectral sub-bands $sb(\delta)_{t,\alpha}$ can be modulated, affecting the spectral-parametric bands (SSBP):

$$sb(\delta)_{t,\alpha} = \{ y(\delta)_{t,\alpha,1};...; y(\delta)_{t,\alpha,\gamma};...; y(\delta)_{t,\alpha,\ell(\delta)_{t,\alpha}} \}$$

where $y(t;\delta)_{\alpha,\gamma}$ is the component with coordinates $(\alpha;\gamma)$ in the t-th spectral array (transformant) with the quantization parameter δ.

The larger the range magnitude, the greater the length $\ell(\delta)_{t,\alpha}$ of the SSBP. As a result, the following occurs:

- reduction in the number of spectral elements for further processing;
- increase in compression level.

This can be explained by the fact that each SSBP $sb(\delta)_{t,\alpha}$ is represented by two parameters: the level $s(\delta)_{t,\alpha}$ and the length $\ell(\delta)_{t,\alpha}$ of the SSBP $sb(\delta)_{t,\alpha}$. It is evident that the ratio function between the number of bits $\log_2 \ell(\delta)_{t,\alpha}$ per length $\ell(\delta)_{t,\alpha}$ of the SSBP and the total number of bits $v(sb(\delta)_{t,\alpha})$ for the representation of spectral elements within such an SSBP exhibits a logarithmic nature:

$$v(sb(\delta)_{t,\alpha}) = bit_y \cdot \ell(\delta)_{t,\alpha}$$

Here, bit_y denotes the number of bits per spectral element in the post-quantization array. Indeed, the evaluations of the growth rates of the number of bits $v(sb(\delta)_{t,\alpha})$ for the sequence of spectral elements within the SSBP and their length $\log_2 \ell(\delta)_{t,\alpha}$ are shown in Table 1.

Table 1. Comparison of growth rates of the number of bits for spectral element sequences within SSBPs and their length $\ell(\delta)_{t,\alpha}$

θ	$\theta \cdot \log_2 \ell(\delta)_{t,\alpha}$, bits	$v(sb(\delta)_{t,\alpha};\theta)$, bits
2	$\log_2 \ell(\delta)_{t,\alpha}$ +1	$2^1 \cdot bit_y \ell(\delta)_{t,\alpha}$
4	$\log_2 \ell(\delta)_{t,\alpha}$ +2	$2^2 \cdot bit_y \ell(\delta)_{t,\alpha}$
8	$\log_2 \ell(\delta)_{t,\alpha}$ +3	$2^3 \cdot bit_y \ell(\delta)_{t,\alpha}$
16	$\log_2 \ell(\delta)_{t,\alpha}$ +4	$2^4 \cdot bit_y \ell(\delta)_{t,\alpha}$

The analysis of the data in Table 1 indicates that the ratio of the growth rates of the number of bits for the two cases demonstrates an exponential trend.

Consequently, the length $\ell(\delta)_{t,\alpha}$ of the SSBP $sb(\delta)_{t,\alpha}$ is treated as a single element, replacing $\ell(\delta)_{t,\alpha}$ individual spectral elements, each requiring bit_y bits. This approach significantly reduces the number of arithmetic operations required for processing.

Thus, for each transformant $Y(\delta)_t$, based on the spectral-parametric representation, two vectors $L(\delta)_t$ and $S(\delta)_t$ are constructed, each corresponding to a specific parameter of the respective SSBP:

$$Y(\delta)_t \rightarrow P(\delta)_t = \{L(\delta)_t;\, S(\delta)_t\} \tag{1}$$

Such vector sets $L(\delta)_t$ and $S(\delta)_t$ can be processed as follows:

- in combined pairs for each SSBP;
- separately for each parameter vector.

However, these approaches do not account for inter-transformant relationships, which may exhibit distinctive characteristics within a group $P(\delta)_T$ of adjacent images $P(\delta)_t$. Therefore, to incorporate the specific features among transformants $P(\delta)_t$ within a group, it is necessary to construct arrays $L(\delta)$ and $S(\delta)$ based on individual parametric vectors of the SPDT description of the transformants:

$$L(\delta) = \{\ell(\delta)_{t,\alpha}\} \;\&\; S(\delta) = \{s(\delta)_{t,\alpha}\}_{\substack{\alpha=\overline{1,\, n(\delta)_{t,sb}} \\ t=\overline{1,\, T}}}$$

where T represents the number of transformants in the group and $n(\delta)_{t,sb}$ denotes the number of SSBPs in the *t*-th transformant based on its SPDT description (or the length of the corresponding parametric vectors $L(\delta)_t$ and $S(t;\delta)$).

However, this introduces conflicts regarding the alignment of lengths $n(\delta)_{t,sb}$ of such parametric vectors $L(\delta)_t$ and $S(\delta)_t$ within the group $P(\delta)_T$ of transformants.

Indeed, the lengths $n(\delta)_{t,sb}$ of the parametric vectors of transformants depend on the complexity of energy redistribution between low- and high-frequency components.

To resolve these conflicts, a procedure for harmonizing transformants based on the characteristics of their SPDT descriptions is performed. This involves redistributing the transformants into clusters $\Omega(\lambda)$.

Clustering of transformants in the SPDT space is defined as the process of partitioning the set of transformants $P(\delta)_t$ into clusters $\Omega(\lambda)$ according to the feature given by the number $n(\delta)_{t,sb}$ of spectral sub-bands $sb(\delta)_{t,\alpha}$ (Fig. 1). Each cluster thus contains transformants that share the same value of this feature, i.e., an identical number of spectral sub-bands $n(\lambda)_{sb}$.

Each cluster $\Omega(\lambda)$ includes only those transformants $P(\xi;\lambda)$ for which the sizes $n(\xi;\lambda)_{sb}$ of their parametric vectors $L(\xi;\lambda)$ and $S(\xi;\lambda)$ in the SPDT description are identical, i.e.:

$$n(\delta)_{t,sb} = n(\xi;\lambda)_{sb} = n(\lambda)_{sb} = const$$

Subsequently, Λ clusters $\Omega(\lambda)$ constructed. The cardinality $|\Omega(\lambda)|$ of each λ-th cluster equals $n(\delta;\lambda)_{tr} = |\Omega(\lambda)|$.

As a result, for the arrays $L(\lambda)$ and $S(\lambda)$:

$$L(\lambda) = \{\ell(\xi;\lambda)_\alpha\}_{\substack{\alpha=\overline{1,\, n(\lambda)_{sb}} \\ \xi=\overline{1,\, n(\lambda)_{tr}}}} \tag{2}$$

$$S(\lambda) = \{s(\xi;\lambda)_\alpha\}_{\substack{\alpha=\overline{1,\, n(\lambda)_{sb}} \\ \xi=\overline{1,\, n(\lambda)_{tr}}}} \tag{3}$$

the parametric vectors $L(\xi;\lambda)$ and $S(\xi;\lambda)$ of the SPDT transformants within a single λ-th cluster are harmonized, resolving conflicts.

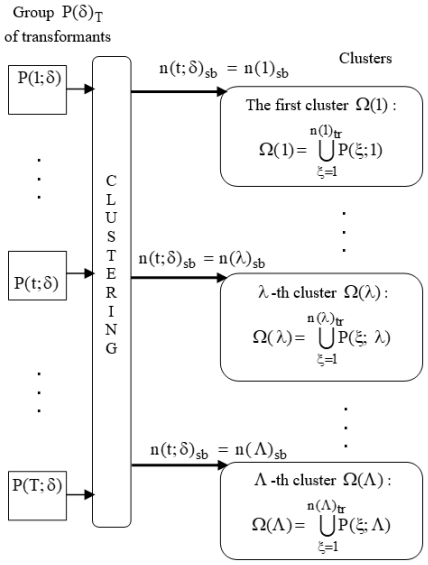

Fig. 1. Schematic of the transformant clustering process in the SPDT space based on the number of SSBPs

This is because the vectors $L(\xi;\lambda)$ and $S(\xi;\lambda)$ within a cluster $\Omega(\lambda)$ have the same number $n(\lambda)_{sb}$ of parameters in the SPDT description of the transformants. In the above expression, the following notation is used: $\ell(\xi;\lambda)_\alpha$ and $s(\xi;\lambda)_\alpha$ are the elements of the vectors $L(\xi;\lambda)$ and $S(\xi;\lambda)$, respectively; $n(\lambda)_{sb}$ and $n(\lambda)_{tr}$ denote the numbers of rows and columns of the arrays and $S(\lambda)$, respectively.

Hence, the arrays $L(\lambda)$ and $S(\lambda)$ can be processed while taking their structural characteristics into account.

These characteristics are proposed to be accounted for as follows:

- determining the lower bounds $\min(L(\lambda)_\alpha)$ and $\min(S(\lambda)_\alpha)$ of the range intervals along the rows $L(\lambda)_\alpha$ and $S(\lambda)_\alpha$ of the constructed two-dimensional arrays $L(\lambda)$ and $S(\lambda)$;
- reducing the range intervals $dip(L(\lambda)_\alpha)$ and $dip(S(\lambda)_\alpha)$ in the columns $L(\xi;\lambda)$ and $S(\xi;\lambda)$ of the two-dimensional parametric arrays $L(\lambda)$ and $S(\lambda)$ by the value of the lower bounds $\min(L(\lambda)_\alpha)$ and $\min(S(\lambda)_\alpha)$ the corresponding rows. That is:

$$dip(L(\lambda)_\alpha) = |L(\lambda)_\alpha| = \underset{\ell(i;\lambda)_\alpha \in L(\lambda)_\alpha}{pow}\{\ell(i;\lambda)_\alpha\} - \min(L(\lambda)_\alpha) \tag{4}$$

$$dip(S(\lambda)_\alpha) = |S(\lambda)_\alpha| = \underset{sign(i;\lambda)_\alpha \in S(\lambda)_\alpha}{pow}\{sign(i;\lambda)_\alpha\} - \min(S(\lambda)_\alpha) \tag{5}$$

$$\min(L(\lambda)_\alpha) = \min_{1 \le i \le n(\lambda)_{tr}}\{\ell(i;\lambda)_\alpha\} \tag{6}$$

$$\min(S(\lambda)_\alpha) = \min_{1 \le i \le n(\lambda)_{tr}}\{sign(i;\lambda)_\alpha\} \tag{7}$$

where $\alpha = \overline{1,\, n(\lambda)_{sb}}$.

In these expressions, the interval values $dip(L(\lambda)_\alpha)$ and $dip(S(\lambda)_\alpha)$ are formed by evaluating the differences between the magnitudes (powers) of $\ell(i;\lambda)_\alpha$ and $s(i;\lambda)_\alpha$ over the regions $\ell(i;\lambda)_\alpha \in L(\lambda)_\alpha$ and $s(i;\lambda)_\alpha \in S(\lambda)_\alpha$ respectively, and the corresponding values of the lower bounds $\min(L(\lambda)_\alpha)$ and $\min(S(\lambda)_\alpha)$. Imposing these constraints creates conditions for reducing structural redundancy during block-positional encoding.

This achieves an additional reduction in redundancy. Indeed, under these conditions, the amount of information $I(P(i;\lambda))$ for the transformant $P(i;\lambda)$ in the SPDT representation decreases after clustering and considering dependencies across slices.

Slices of the SPDT space are defined as the rows of the arrays $L(\lambda)$ and $S(\lambda)$. Hence, the corresponding slices at position α are given by:

$$L(\lambda)_\alpha = \{\ell(1;\lambda)_\alpha;...;\ell(\xi;\lambda)_\alpha;...;\ell(n(\lambda)_{tr};\lambda)_\alpha\}$$
$$S(\lambda)_\alpha = \{s(1;\lambda)_\alpha;...;s(\xi;\lambda)_\alpha;...;s(n(\lambda)_{tr};\lambda)_\alpha\}$$
$$\alpha = \overline{1,\, n(\lambda)_{sb}}$$

In general, the amount of information $I(P(i;\lambda))$ is determined by the range of intervals for the variations in the parametric vectors $\bar{L}(i;\lambda)$ and $\bar{S}(i;\lambda)$:

$$I(P(i;\lambda)) = n(i;\lambda)_{sb} \times (\ell og_2\, dip(L(\lambda)_\alpha) + \ell og_2 dip(S(\lambda)_\alpha)$$

or

$$I(P(i;\lambda)) = n(i;\lambda)_{sb} \times$$
$$\times (\ell og_2 (\underset{\ell(i;\lambda)_\alpha \in L(\lambda)_\alpha}{pow} \{\ell(i;\lambda)_\alpha\} - \min(L(\lambda)_\alpha)) +$$
$$+ \ell og_2 (\underset{sign(i;\lambda)_\alpha \in S(\lambda)_\alpha}{pow} \{sign(i;\lambda)_\alpha\} - \min(S(\lambda)_\alpha))$$

The above expressions make it possible to determine the number of bits (bit volume) required for a compact representation of the SPDT description vectors of transformants within a cluster, while accounting for additional slice-level structural dependencies.

This, in turn, allows the evaluation of the amount of information $I(loc(i;\lambda))$ contained in a single spectral sub-band $s(i)_\alpha$:

$$I(loc(i;\lambda)) = I(P(i;\lambda)) / n(i;\lambda)_{sb} =$$
$$= \ell og_2\, dip(L(\lambda)_\alpha) \cdot \ell og_2 dip(S(\lambda)_\alpha)$$

Here, $\ell og_2\, dip(L(\lambda)_\alpha)$ and $\ell og_2 dip(S(\lambda)_\alpha)$ denote the numbers of bits required to encode the values $dip(L(\lambda)_\alpha)$ and $dip(S(\lambda)_\alpha)$, respectively.

The derived relationship provides a framework for evaluating the amount of information while accounting for additional dependencies in the slices of two-dimensional parametric SPDT arrays within a cluster. This outcome is directly linked to the narrowing of the interval range $dip(\bar{L}(i;\lambda))$, $dip(\bar{S}(i;\lambda))$ of the parameters $\ell(i;\lambda)_\alpha$, $sign(i;\lambda)_\alpha$, enabling the elimination of corresponding redundancy. The amount of redundancy $r(i;\lambda)$ comparing situations before and after applying constraints along slice directions, can be calculated as:

$$r(i;\lambda) = 100 \cdot (1 - \frac{\ell og_2 dip(\bar{L}(i;\lambda)) \cdot diap(\bar{S}(i;\lambda))}{\ell og_2 dip(L(i;\lambda)) \cdot dip(S(i;\lambda))})\%$$
$$r(i;\lambda) > 0$$

It can be concluded that evaluating the level of informativeness of the cluster transformants in SPDT representation, while considering interval range characteristics within slices, demonstrates the potential for further redundancy reduction.

Thus, there is a clear need to develop a method for compressing two-dimensional parametric arrays of cluster transformants, considering the unique features within their groups.

3. Development of the method of block coding transformants by structural components

The space formed after accounting for the characteristics along the slices of two-dimensional parametric arrays within clusters is referred to as the normalized space. The normalized variants $\bar{\ell}(\xi;\lambda)_\alpha$ and $\bar{s}(\xi;\lambda)_\alpha$ for each parametric characteristic of the SPDT representation of transformants are computed using a differential scheme, which can be represented by the following expressions:

$$\bar{\ell}(i;\lambda)_\alpha = \ell(i;\lambda)_\alpha - \min(L(\lambda)_\alpha)$$
$$\bar{s}(i;\lambda)_\alpha = s(i;\lambda)_\alpha - \min(S(\lambda)_\alpha)$$

After normalization, the components $\bar{L}(\xi;\lambda)$ and $\bar{S}(\xi;\lambda)$ of the SPDT representation of the transformants are adjusted by reducing the range of values by $\min(L(\lambda)_\alpha)$ and $\min(S(\lambda)_\alpha)$, respectively, as follows:

$$\bar{L}(\xi;\lambda) = \{\bar{\ell}(\xi;\lambda)_\alpha\}_{\xi = \overline{1,\,|\Omega(\lambda)|}} \quad (8)$$

$$\bar{S}(\xi;\lambda) = \{\overline{sign}(\xi;\lambda)_\alpha\}_{\xi = \overline{1,\,|\Omega(\lambda)|}} \quad (9)$$

Here, the values $\min(L(\lambda)_\alpha)$ and $\min(S(\lambda)_\alpha)$ are computed according to expressions (6) and (7).

To eliminate redundancy, it may be necessary to account for the characteristics of cluster slices during the calculation of weight coefficients. Additionally, to increase the compression ratio, it is proposed to generate codes directly for each parametric vector. These codes belong to the class of block codes. Thus, during encoding, block-parametric codes $C_{\bar{L}}(\xi;\lambda)$ and $C_{\bar{S}}(\xi;\lambda)$ will be constructed. Such encoding is performed separately within each λ-th cluster for $i = \overline{1,\, n(\lambda)_{tr}}$:

$$C_{\bar{L}}(\xi;\lambda) = \underset{V_{\bar{L}}(\xi;\lambda)}{bin} (\sum_{\alpha=1}^{n(\lambda)_{sb}} \bar{\ell}(i;\lambda)_\alpha \cdot \psi(\bar{\ell}(i;\lambda))_\alpha) =$$
$$= \underset{V_{\bar{L}}(\xi;\lambda)}{bin} (\sum_{\alpha=1}^{n(\lambda)_{sb}} \bar{\ell}(i;\lambda)_\alpha \cdot dip(\bar{L}(i;\lambda)^{(1)})^{n(\lambda)_{sb}-\alpha})$$
$$C_{\bar{S}}(\xi;\lambda) = \underset{V_{\bar{S}}(\xi;\lambda)}{bin} (\sum_{\alpha=1}^{n(\lambda)_{sb}} \bar{s}(i;\lambda)_\alpha \cdot \psi(\bar{s}(i;\lambda))_\alpha) =$$
$$= \underset{V_{\bar{S}}(\xi;\lambda)}{bin} (\sum_{\alpha=1}^{n(\lambda)_{sb}} \bar{s}(i;\lambda)_\alpha \cdot dip(S(i;\lambda)^{(1)})^{n(\lambda)_{sb}-\alpha})$$

The following notation is used in these expressions:

1) $V_{\bar{L}}(\xi;\lambda)$ and $V_{\bar{S}}(\xi;\lambda)$ are the current bit-lengths of the binary numbers (codes) corresponding to $C_{\bar{L}}(\xi;\lambda)$ and $C_{\bar{S}}(\xi;\lambda)$, respectively;
2) $\underset{V_{\bar{L}}(\xi;\lambda)}{bin}$ and $\underset{V_{\bar{S}}(\xi;\lambda)}{bin}$ are the functionals used to form the block codes $C_{\bar{L}}(\xi;\lambda)$ and $C_{\bar{S}}(\xi;\lambda)$ within code word lengths equal to $V_{\bar{L}}(\xi;\lambda)$ and $V_{\bar{S}}(\xi;\lambda)$, respectively;

3) $\psi(\overline{\ell}(i;\lambda))_\alpha$ and $\psi(\overline{s}(i;\lambda))_\alpha$ are weighting coefficients for the elements $\overline{\ell}(\xi;\lambda)_\alpha$ and $\overline{s}(\xi;\lambda)_\alpha$ of the normalized space for each parametric characteristic of the SPDT. They specify the contribution (weight) of each element in the parametric–positional space during block-code formation. The values $\psi(\overline{\ell}(i;\lambda))_\alpha$ and $\psi(\overline{s}(i;\lambda))_\alpha$ are obtained as cumulative products of the normalized intervals of the less significant elements of the parametric-positional numbers. Therefore, the weighting coefficients for the α -th elements of the parametric–positional numbers (columns of $\overline{L}(\xi;\lambda)$ and $\overline{S}(\xi;\lambda)$) are computed as:

$$\psi(\overline{\ell}(i;\lambda))_\alpha = diap(\overline{L}(i;\lambda)^{(1)})^{n(\lambda)_{sb}-\alpha}$$

$$\psi(\overline{s}(i;\lambda))_\alpha = diap(S(i;\lambda)^{(1)})^{n(\lambda)_{sb}-\alpha}$$

Here, $n(\lambda)_{sb}-\alpha$ is the number of less significant elements in the parametric–positional number.

Accordingly, for each cluster, two code sequences $C_{\overline{L}}(\lambda)$ and $C_{\overline{S}}(\lambda)$ are generated for each of the parametric vectors of the SPDT representation of the transformant $P(\xi;\lambda)$. Thus, for the λ -th cluster, we obtain:

$$P(\lambda):$$

$$C_{\overline{L}}(\lambda) = \{C_{\overline{L}}(1;\lambda);...;C_{\overline{L}}(i;\lambda);...;C_{\overline{L}}(n(\lambda)_{tr};\lambda)\}$$

$$C_{\overline{S}}(\lambda) = \{C_{\overline{S}}(1;\lambda);...;C_{\overline{S}}(i;\lambda);...;C_{\overline{S}}(n(\lambda)_{tr};\lambda)\}$$

Thus, further development of the image compression method is achieved through block coding of the parametric vectors of the transformant's SPDT representation within individual clusters, with variation normalization incorporated. The method is constructed with weight calculation, taking into account constraints on the range of changes in the values of corresponding components along the SPS slices.

The structural-functional block diagram of block-parametric coding of transformants in a cluster within the SPDT description is presented in Fig. 2.

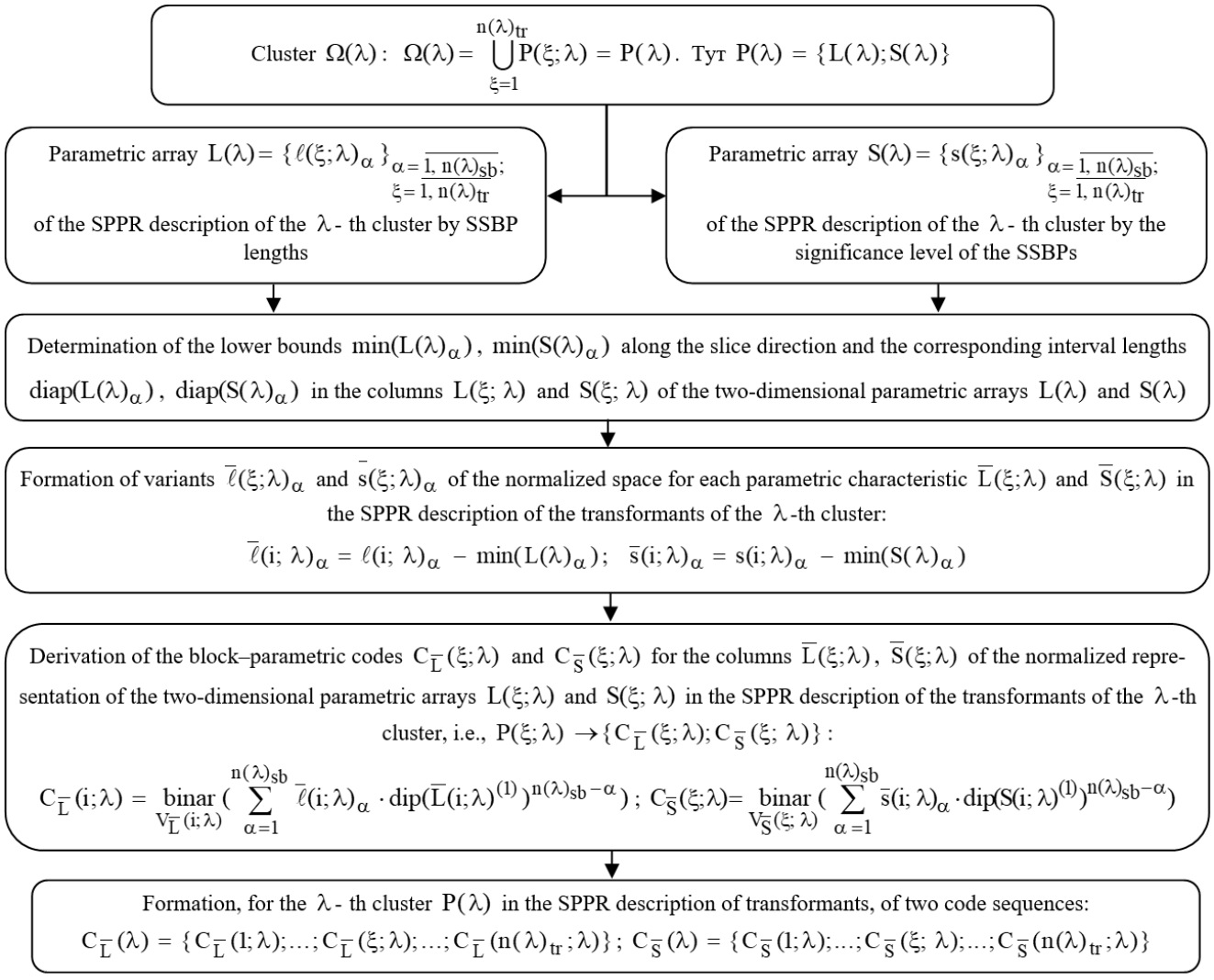

Fig. 2. Structural-functional block diagram of block–parametric coding of transformants in a cluster within the SPDT description

At the same time, the resulting codes $C_{\overline{L}}(\xi;\lambda)$ and $C_{\overline{S}}(\xi;\lambda)$ are binary numbers whose required code word lengths $V_{\overline{L}}(\xi;\lambda)$ and $V_{\overline{S}}(\xi;\lambda)$ remain undefined. However, specifying these lengths is essential for the final determination of the compression ratio (i.e., the reduction in bit budget).

Therefore, a key issue in ensuring both the desired compression performance and the fidelity of the reconstructed data is the development of a ***strategy for determining the number of bits*** allocated to the lengths $V_{\overline{L}}(\xi;\lambda)$ and $V_{\overline{S}}(\xi;\lambda)$ of the codes $C_{\overline{L}}(\xi;\lambda)$ and $C_{\overline{S}}(\xi;\lambda)$ that represent the structural components of SPDT for $\lambda = \overline{1,\Lambda}$.

In developing the coding strategy, it is essential to consider:

- on the one hand, the uniformity of the structural components of the SPDT for the sequence of transformants within each cluster along the respective SPS slices $\bar{L}(\lambda)_{\alpha}$, $\bar{S}(\lambda)_{\alpha}$;
- on the other hand, the potential heterogeneity in the values of the components $\overline{\ell}(\xi;\lambda)_{\alpha}$, $\overline{sign}(\xi;\lambda)_{\alpha}$ along the respective structural components $\bar{L}(\xi;\lambda)$, $\bar{S}(\xi;\lambda)$ of each SPDT description.

The following options for code definition based on the values of $V_{\bar{L}}(\xi;\lambda)$, $V_{\bar{S}}(\xi;\lambda)$ are possible:

1) First option: Determining the values of $V_{\bar{L}}(\xi;\lambda)$ and $V_{\bar{S}}(\xi;\lambda)$ based on the principle of the minimally sufficient number of bits to represent the values $[C_{\bar{L}}(\xi;\lambda)]_{10}$ and $[C_{\bar{S}}(\xi;\lambda)]_{10}$ in binary form, as follows:

$$ {}_1V_{\bar{L}}(\xi;\lambda) = [\log_2[C_{\bar{L}}(\xi;\lambda)]_{10}] + 1 $$

$$ {}_1VC_{\bar{S}}(\xi;\lambda) = [\log_2[C_{\bar{S}}(\xi;\lambda)]_{10}] + 1 $$

However, this approach does not account for the non-uniformity of the values $[C_{\bar{L}}(\xi;\lambda)]_{10}$ and $[C_{\bar{S}}(\xi;\lambda)]_{10}$ across different transformants within the cluster.

2) Second option: Utilizing the positional rule to define the codes, incorporating weight characteristics $\psi(\overline{\ell}(\xi;\lambda))_{\alpha}$ and $\psi(\overline{s}(\xi;\lambda))_{\alpha}$. This rule involves setting an upper limit for the values of $[C_{\bar{L}}(\xi;\lambda)]_{10}$ and $[C_{\bar{S}}(\xi;\lambda)]_{10}$, determined by the respective ranges $diap(\bar{L}(\xi;\lambda))$, $diap(\bar{S}(\xi;\lambda))$. For this option, the lengths ${}_2V_{\bar{L}}(\xi;\lambda)$ and ${}_2V_{\bar{S}}(\xi;\lambda)$ of the codes $C_{\bar{L}}(\xi;\lambda)$ and $C_{\bar{S}}(\xi;\lambda)$ are computed as:

$$ {}_2V_{\bar{L}}(\xi;\lambda) = n(\lambda)_{sb} \cdot \ell og_2 dip(\bar{L}(\xi;\lambda)) $$

$$ {}_2V_{\bar{S}}(\xi;\lambda) = n(\lambda)_{sb} \cdot \ell og_2 dip(\bar{S}(\xi;\lambda)) $$

However, this approach does not account for scenarios where the minimally enough bits is significantly smaller than the number of bits determined by the positional rule, i.e.:

$$ {}_1V_{\bar{L}}(\xi;\lambda) \lll n(\lambda)_{sb} \cdot \ell og_2 dip(\bar{L}(\xi;\lambda)) $$

$$ {}_1V_{\bar{S}}(\xi;\lambda) \lll n(\lambda)_{sb} \cdot \ell og_2 dip(\bar{S}(\xi;\lambda)) $$

In such cases, code definition based on the second option results in code redundancy. To eliminate this drawback, the third option for constructing the code definition strategy is proposed

3) Third option: The code definition is based on the ***technology of locally monotonic code formation***. This approach utilizes markers $dip(V_{\bar{L}}(\lambda))$ and $dip(V_{\bar{S}}(\lambda))$, which carry information about the lengths ${}_3V_{\bar{L}}(\xi;\lambda)$ and ${}_3V_{\bar{S}}(\xi;\lambda)$ of the codes $C_{\bar{L}}(\xi;\lambda)$ and $C_{\bar{S}}(\xi;\lambda)$. In this method, the lengths ${}_3V_{\bar{L}}(\xi;\lambda)$ and ${}_3V_{\bar{S}}(\xi;\lambda)$ are determined according to the rule of local monotonicity, expressed as

$$ {}_3V_{\bar{L}}(\xi;\lambda) = {}_3V_{\bar{L}}(\lambda) = \max_{1\le\xi\le n(\lambda)_{tr}} \{{}_1V_{\bar{L}}(\xi;\lambda)\} $$

$$ {}_3V_{\bar{S}}(\xi;\lambda) = {}_3V_{\bar{S}}(\lambda) = \max_{1\le\xi\le n(\lambda)_{tr}} \{{}_1V_{\bar{S}}(\xi;\lambda)\} $$

Accordingly, each marker contains the following information:

$$ dip(V_{\bar{L}}(\lambda)) := {}_3V_{\bar{L}}(\xi;\lambda) $$

$$ dip(V_{\bar{S}}(\lambda)) := {}_3V_{\bar{S}}(\xi;\lambda) $$

In the binary representation of the markers themselves, the number of bits $|dip(V_{\bar{L}}(\lambda))|$ and $|dip(V_{\bar{S}}(\lambda)|$ is allocated based on one of the following principles:

1) maximum Value Principle: This principle considers the largest values $\max_{1\le\xi\le n(\lambda)_{tr}} dip(\bar{L}(\xi;\lambda))$ and $\max_{1\le\xi\le n(\lambda)_{tr}} dip(\bar{S}(\xi;\lambda))$ for the parameters $dip(\bar{L}(\xi;\lambda))$ and $dip(\bar{S}(\xi;\lambda))$ across all structural components of the SPDT within the cluster:

$$ |dip(V_{\bar{L}}(\xi;\lambda))| = \max_{1\le\xi\le n(\lambda)_{tr}} {}_2V_{\bar{L}}(\xi;\lambda)) $$

$$ |dip(V_{\bar{S}}(\xi;\lambda))| = \max_{1\le\xi\le n(\lambda)_{tr}} {}_2V_{\bar{S}}(\xi;\lambda) $$

2) uniform Code Principle: In this case, the number of bits V_{mar} allocated for the binary description of markers is uniform and constant throughout the processing of the entire sequence of video fragments. Thus:

$$ |dip(V_{\bar{L}}(\lambda))| = |dip(V_{\bar{S}}(\lambda))| = V_{mar} $$

3) adaptive Principle: The essence of this approach lies in selecting the bit length of markers $V(n(\lambda)_{sb})_L$ and $V(n(\lambda)_{sb})_S$ separately for each structural component $\bar{L}(\xi;\lambda)$ and $\bar{S}(\xi;\lambda)$ of the SPDT, depending on the number $n(\lambda)_{sb}$ of LCMs for the current λ-th cluster. The following expressions are used:

$$ V(n(\lambda)_{sb})_L = n(\lambda)_{sb} \cdot \ell og_2(n^2 - n(\lambda)_{sb}) \quad (10) $$

$$ V(n(\lambda)_{sb})_S = n(\lambda)_{sb} \cdot bit_y \quad (11) $$

Here: $n(\lambda)_{sb}$ is the number of spectral sub-bands formed during the SPDT description of the transformants of the λ-th cluster; bit_y is the maximum number of bits used to represent transformant components after quantization (most often $b_y = 8$ bits); n is the linear size of the transformant; $(n^2 - n(\lambda)_{sb})$ is the maximum possible length of a spectral sub-band under the formation of $n(\delta;\lambda)_{sb}$ SSBPs.

The physical meaning of expression (10) is that the marker length $V(n(\lambda)_{sb})_L$ is determined as the number of bits required to represent the maximum possible value for the columns $\bar{L}(\xi;\lambda)$ of the array $\bar{L}(\lambda)$. That is:

$$ 2^{V(n(\lambda)_{sb})_L} = (n^2 - n(\lambda)_{sb})^{n(\lambda)_{sb}} $$

Expression (11) has an analogous meaning. Specifically, the quantity $n(\lambda)_{sb} \cdot bit_y$ is the maximum possible value of the length $V_{\bar{S}}(\xi;\lambda)$ of the code $C_{\bar{L}}(\xi;\lambda)$ for the columns $\bar{S}(\xi;\lambda)$ of the normalized array $\bar{S}(\delta;\lambda)$.

Consequently:

$$ |diap(V_{\bar{L}}(\lambda))| = V(n(\lambda)_{sb})_L $$

$$ |diap(V_{\bar{S}}(\lambda)| = V(n(\lambda)_{sb})_S $$

This approach enables the following benefits:

- for the First Principle: It reduces the amount of auxiliary information, and the computational efforts required to determine the bit length of markers for each cluster;
- for the Second Principle: It decreases the number of bits needed to represent the markers of binary block codes for each cluster.

In this context, the number of bits used for the binary representation of markers is selected adaptively based on the structural characteristics of each cluster.

A structural–functional block diagram of the locally monotonic coding method with adaptive consideration of the structural parameters of a transformant cluster in the SPDT description is shown in Fig. 3.

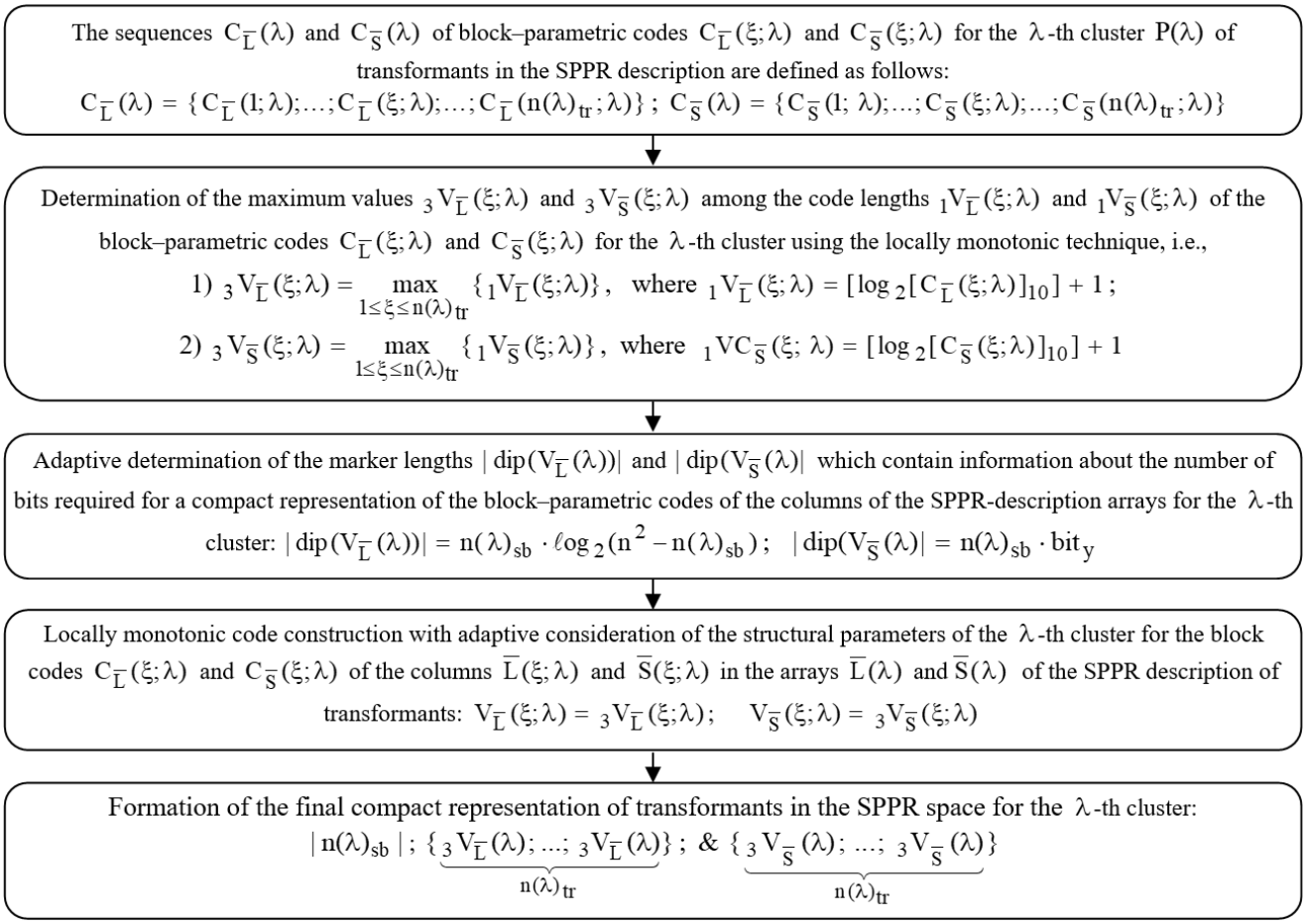

Fig. 3. Structural-functional block diagram of the locally monotonic coding method with adaptive consideration of the structural parameters of a transformant cluster in the SPDT description

Therefore, ***it is proposed*** to form local markers for each cluster. The functional purpose of these markers is to delineate the boundaries of:

- coding constructs $C_{\bar{L}}(\xi;\lambda)$, $C_{\bar{S}}(\xi;\lambda)$ for the structural components $\bar{L}(\xi;\lambda)$, $\bar{S}(\xi;\lambda)$ of individual transformants $P(\xi;\lambda)$ within the overall cluster stream;
- coding constructs $C_{\bar{L}}(\lambda)$, $C_{\bar{S}}(\lambda)$ for adjacent clusters.

Let us consider the generalized coded representation of the sequence $P(\delta)_T$ of transformants $P(\delta)_t$. The overall coding structure C_T for the sequence of transformants $P(\delta)_T$, developed using the proposed coding technology, includes both a service part $C(T)_{\mathrm{sec}}$ and an informational part $C(T)_{\mathrm{inf}}$:

$$C_T = C(T)_{\mathrm{sec}} + C(T)_{\mathrm{inf}}$$

When considering the cluster-based structure of the developed coding process for a sequence of video fragments, we derive the following:

1) For the service part $C(T)_{\mathrm{sec}}$ of the overall coding sequence C_T, the following information is included:

Marker λ of the cluster of transformants, which are homogeneous in terms of the number $n(\lambda)_{sb}$ of LCMs in their spectral-parametric description.

Number $n(\lambda)_{sb}$ of LCMs (or the number of SSPs) in each cluster, which also serve as markers indicating the transformant's membership in a specific cluster.

Markers $M(\bar{L}(\xi;\lambda))$, $M(\bar{S}(\xi;\lambda))$, which convey information about the number ${}_3V_{\bar{L}}(\xi;\lambda)$, ${}_3V_{\bar{S}}(\xi;\lambda)$ of bits for block codes $C_{\bar{L}}(\xi;\lambda)$ and $C_{\bar{S}}(\xi;\lambda)$ for each cluster.

Lengths $dip(\bar{L}(\xi;\lambda))$ and $dip(\bar{S}(\xi;\lambda))$ of the ranges defining the component values in the structural components $\bar{L}(\xi;\lambda)$ and $\bar{S}(\xi;\lambda)$ of each SPDT $P(\xi;\lambda)$ for the λ-th cluster.

Lower bounds $\min(L(\lambda)_\alpha)$ and $\min(S(\lambda)_\alpha)$ of the ranges defining the components $\bar{\ell}(\xi;\lambda)_\alpha$ and $\bar{s}(\xi;\lambda)_\alpha$ in the directions of the respective SPC slices $L(\lambda)_\alpha$ and $S(\lambda)_\alpha$ of the clusters.

Parameter δ of the quantization strategy for the spectral component array.

2) For the informational part $C(T)_{\mathrm{inf}}$ of the overall coding sequence C_T. For each transformant in the λ-th cluster, two block codes are constructed corresponding to the structural components: $C_{\bar{L}}(\xi;\lambda)$ and $C_{\bar{S}}(\xi;\lambda)$. For the entire sequence $P(\lambda)$ of transformants $P(\xi;\lambda)$ in the spectral-parametric description across all clusters, two sequences $C(\bar{L}(\Lambda))$ and $C(\bar{S}(\Lambda))$ of binary block codes are constructed corresponding to the structural components:

$$C(\bar{L}(\Lambda)) = \{C_{\bar{L}}(1;\lambda);\ldots;C_{\bar{L}}(n(\lambda)_{tr};\lambda)\}$$

$$C(\bar{S}(\Lambda)) = \{C_{\bar{S}}(1;\lambda);\ldots;;C_{\bar{S}}(n(\lambda)_{tr};\lambda)\}$$

4. Image volume estimation using compression technologies

A significant number of existing compression technologies are based on the principle of coding individual segments. Therefore, to facilitate a more accurate comparison of the characteristics of different methods, it is necessary to determine the average bit volume of the transformant in SPDT for the developed method. We denote this value as $V_{\delta,1}$:

$$V_{\delta,1} = \frac{V_T}{T}$$

This quantity is fundamental for determining such characteristics as the compression ratio r_{cmp} and the average number of bits per pixel (bpp).

To assess visual reconstruction quality, the peak signal-to-noise ratio (PSNR) and the structural similarity index (SSIM) are used.

The compression performance of the proposed approach is evaluated through experimental studies using a software prototype. Reference video sequences are selected from recommended international datasets (TED 2013) [23]. Within each video frame, segments are categorized by complexity level. The PSNR and SSIM characteristics are controlled by varying the quantization level. Reconstruction quality is assessed at PSNR values of 26 and 38 dB. This choice is motivated by the fact that these PSNR levels correspond to the required quality for video fragments of medium and high informational significance, respectively.

Under the proposed method (SSPO), the complexity of video fragments is characterized by the parameter $n(\delta;\lambda)_{sb}$. This parameter specifies the number of spectral sub-bands produced when forming the SPDT description of a transformant. In the general case, its value depends on:

- the degree to which the original images contain fine details;
- the value of the normalized correlation coefficient r;
- the quantization mode applied to the transformants prior to SPDT construction.

The proposed method addresses the part of the overall compression pipeline related to generating transformants (i.e., constructing the spectral representation of video fragments) and encoding them. Therefore, the method (SSPO) is intended to be integrated into a complete compression framework. As a baseline for integration, we consider compression platforms that include a transform stage such as the discrete cosine transform or wavelet transforms. This category includes modern compression technologies that incorporate modified variants of the JPEG platform architecture, such as JPEG XL, HEVC/H.265 intra, and VVC. In this case, the difference between the conventional approaches and the proposed method concerns primarily the processing stages for sequences of transformed video fragments in the spectral or spectral–temporal domain.

Accordingly, for existing approaches, two principal options are commonly used to process transformed video fragments:

1) The first option relies on entropy coding based on modified Huffman tables and ANS (asymmetric numeral systems) coding tables. This approach is implemented in JPEG XL, WebP, and HEVC/H.265 intra [9, 28];
2) The second option combines entropy coding with techniques for constructing dynamic context models. In this case, integer arithmetic coding methods are employed. This approach is implemented in JPEG 2000, JPEG XR, and VVC [12, 27].

Another class of modern compression platforms is based on artificial intelligence models. An example is the JPEG AI platform [20], which uses semantic processing models built on the Transformer architecture [19, 25]. Transformer-based models can be used in conjunction with the proposed method. For instance, they may be applied to pre-process video segments in order to identify the most informative ones. However, such approaches are constrained in on-board deployments due to the complexity of implementing the compression process. In addition, AI-based compression methods often yield lower reconstruction quality than classical standards at comparable compression levels. For example, at PSNR = 30 dB, the compression ratio typically does not exceed a factor of five for content-rich video sequences.

Therefore, JPEG XL and JPEG XR are selected for further comparison with the proposed method (SSPO).

The choice of these technologies is motivated by the following considerations:

- they employ standard pre-processing mechanisms: transform coding based on the discrete cosine transform and the construction of the spectral-parametric description components of transformants;
- they support compression in a controlled loss mode, ensuring acceptable visual quality of the decompressed images;
- they use quantization strategies with adjustable parameters to control the PSNR level.
- they operate in a symmetric transform mode, where the computational effort for encoding is comparable to that for reconstruction.

The comparative evaluation is performed by plotting the dependence of the compression ratio r_{cmp} on the PSNR-based reconstruction quality. The corresponding plots are shown in Fig. 4. To identify characteristic trends, three types of video fragments are processed. These types are defined by the quantitative parameter $n(\delta;\lambda)_{sb}$, which is key for clustering transformants in the SPDT description.

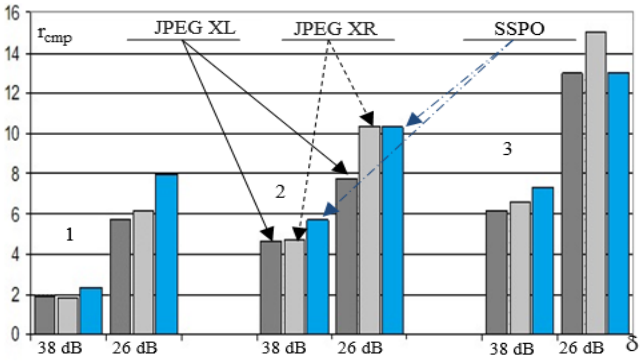

Fig. 4. Dependence of r_{cmp} on the SPDT parametr $n(\delta;\lambda)_{sb}$ for different compression methods at PSNR 26 and 38 dB

Accordingly, the comparative evaluation is carried out as a function of:

1) SPDT-transformant parameters defined by the number of sub-bands $n(\delta;\lambda)_{sb}$ The following ranges are used for $n(\delta;\lambda)_{sb}$:
   - structurally significant SPDT: $14 \le n(\delta;\lambda)_{sb}$;
   - structurally complex SPDT: $6 \le n(\delta;\lambda)_{sb} \le 13$;
   - structurally simple SPDT: $n(\delta;\lambda)_{sb} \le 5$.
2) parameters of the quantization strategy. Two operating points are considered, corresponding to PSNR levels of PSNR = 26 dB and PSNR = 38 dB.

From the analysis of the diagrams in Figure 4, the following conclusions can be drawn:

1) for significant SPDT transformants (large values of the parameter $n(\delta;\lambda)_{sb}$) with quantization parameters forming PSNR levels between 26 and 38 dB, the proposed SSPO method demonstrates superior compression ratios. The gain over the compared methods, depending on the PSNR level, is: JPEG XL – 15 to 21%; JPEG XR –14 to 18%;

a)


b)


c)


Fig. 5. Reconstructed reference video frame: (a) original; (b) compression mode with PSNR = 38 dB; (c) compression mode with PSNR=26dB

2) the SSPO technology provides an advantage of 11% to 15% in compressed image formation at 38 dB, regardless of the number of spectral sub-bands in the spectral-parametric description of the transformants.

These results are attributed to the following factors:

- for structurally significant SPDT transformants, the statistical properties of the transformants are non-stationary and vary sharply across the sequence. This reduces the efficiency of statistical coding technologies. Specifically, in JPEG XL, compression performance may degrade due to an increased number of local components in the SPDT description;
- as PSNR increases, the statistical properties of the transformant components stabilize. The probability distribution of the component occurrences approaches uniformity, and the number of zero components decreases.

The results of reconstructing the reference video frame at different PSNR levels are presented in Fig. 5.

Based on the examples of reconstructed frames at varying PSNR values, it can be concluded that, at a compression setting of PSNR = 38 dB, no visually perceptible quality degradation is observed for information-rich video segments. At PSNR = 26 dB, no significant integrity loss is observed for low-information video fragments.

Limitations of the proposed coding method:

1) It requires a dedicated pre-processing stage that performs the discrete cosine transform to construct the spectral domain.
2) It is limited to processing segments from static video frames.

5. Conclusions

1. A method for locally monotonic code determination for binary block codes in the differential-normalized space of the structural components of the spectral-parametric description of clustered transformants was developed. This method utilizes fixed-length markers and is based on defining intervals within

the domain of arguments for block coding functions. It ensures the required level of integrity for restored video fragments by creating conditions for one-to-one transformations in the formation of codegrams.

2. A method for coding the lengths of binary block code markers for the SPDT components was proposed. The method is grounded in an adaptive principle, which determines the bit length of markers in the cluster code sequence separately for each structural component of the SPDT, depending on their complexity. This approach offers the following advantages:

- reduction in the amount of service information and computational operations required to determine the bit length of markers for each cluster;
- decrease in the number of bits required to represent the markers of binary block codes for each cluster.

3. An evaluation of the bit consumption required for the codegram of the compressed representation of a sequence of clustered SPDT-transformants was carried out using the developed method. This evaluation was performed as a function of the clustering parameter of the transformants under a given PSNR level. The findings are as follows:

1) the bit consumption for a single compressed SPDT-transformant varies with the value of the clustering parameter $n(\delta;\lambda)_{sb}$:

- for quantization parameters ensuring PSNR = 38 dB, the bit consumption ranges from 68 to 227 bits/transformant;
- for quantization parameters ensuring PSNR = 26 dB the bit consumption ranges from 35 to 60 bits/transformant;

2) The implementation of the quantization strategy allows for further reduction in bit consumption for compressed SPDT-transformants. Increasing the quantization level, which decreases PSNR by 10 dB from PSNR = 38 dB to PSNR = 26 dB, results in a reduction in bit consumption for a compressed SPDT-transformant by an average of 1.5 to 3.7 times;

3) a comparative analysis of the compression ratio for the developed method and existing methods revealed:

- for significant SPDT-transformants with quantization parameters forming a PSNR level from 26 to 38 dB, the developed SSPC method achieves a superior compression ratio. The advantage, depending on the PSNR level, is as follows: JPEG XL – from 16 to 20%; JPEG XR – from 15 to 17%;
- the SSPC technology provides an advantage of 12% to 16% in generating compressed images at a PSNR level of 38 dB for various numbers of spectral sub-bands in the spectral-parametric description of transformants.

References

[1] Aouladhadj, D., Kpre, E., Deniau, V., Kharchouf, A., Gransart, C., & Gaquière, C. (2023). Drone Detection and Tracking Using RF Identification Signals. *Sensors*, *23*(17), 7650. https://doi.org/10.3390/s23177650

[2] Barannik, D., & Barannik, V. (2022). Steganographic Coding Technology for Hiding Information in Infocommunication Systems of Critical Infrastructure. *2022 IEEE 4th International Conference on Advanced Trends in Information Theory (ATIT)*, 88–91. https://doi.org/10.1109/ATIT58178.2022.10024185

[3] Barannik, V., Barannik, D., Fustii, V., & Parkhomenko, M. (2019). Evaluation of Effectiveness of Masking Methods of Aerial Photographs. *2019 3rd International Conference on Advanced Information and Communications Technologies (AICT)*, 415–418. https://doi.org/10.1109/AIACT.2019.8847820

[4] Barannik, V., Shulgin, S., Barannik, N., & Barannik, V. (2022). Method of Coding Subbands of Non-Homogeneous Spectrum of Video Segments in Uneven Diagonal Space. *2022 IEEE 4th International Conference on Advanced Trends in Information Theory (ATIT)*, 72–75. https://doi.org/10.1109/ATIT58178.2022.10024236

[5] Bondžulić, B., Stojanović, N., Petrović, V., Pavlović, B., & Miličević, Z. (2021). Efficient Prediction of the First Just Noticeable Difference Point for JPEG Compressed Images. *Acta Polytechnica Hungarica*, *18*(8), 201–220. https://doi.org/10.12700/APH.18.8.2021.8.11

[6] Bross, B., Wang, Y.-K., Ye, Y., Liu, S., Chen, J., Sullivan, G. J., & Ohm, J.-R. (2021). Overview of the Versatile Video Coding (VVC) Standard and its Applications. *IEEE Transactions on Circuits and Systems for Video Technology*, *31*(10), 3736–3764. https://doi.org/10.1109/TCSVT.2021.3101953

[7] Chen, T., Liu, H., Ma, Z., Shen, Q., Cao, X., & Wang, Y. (2021). End-to-End Learnt Image Compression via Non-Local Attention Optimization and Improved Context Modeling. *IEEE Transactions on Image Processing*, *30*, 3179–3191. https://doi.org/10.1109/TIP.2021.3058615

[8] Dua, Y., Kumar, V., & Singh, R. S. (2020). Comprehensive review of hyperspectral image compression algorithms. *Optical Engineering*, *59*(09). https://doi.org/10.1117/1.OE.59.9.090902

[9] Duda, J. (2013). *Asymmetric numeral systems: Entropy coding combining speed of Huffman coding with compression rate of arithmetic coding* (Version 2). arXiv. https://doi.org/10.48550/ARXIV.1311.2540

[10] Fu, C.-M., Alshina, E., Alshin, A., Huang, Y.-W., Chen, C.-Y., Tsai, C.-Y., Hsu, C.-W., Lei, S.-M., Park, J.-H., & Han, W.-J. (2012). Sample Adaptive Offset in the HEVC Standard. *IEEE Transactions on Circuits and Systems for Video Technology*, *22*(12), 1755–1764. https://doi.org/10.1109/TCSVT.2012.2221529

[11] Hazowary, P., Dutta, S. K., & Subadar, R. (2022). A Comparison of Image Compression Techniques Over Wireless Fading Channel. In H. K. D. Sarma, V. E. Balas, B. Bhuyan, & N. Dutta (Eds), *Contemporary Issues in Communication, Cloud and Big Data Analytics* (Vol. 281, pp. 241–249). Springer Singapore. https://doi.org/10.1007/978-981-16-4244-9_19

[12] Helin, H., Tolonen, T., Ylinen, O., Tolonen, P., Napankangas, J., & Isola, J. (2018). Optimized JPEG 2000 Compression for Efficient Storage of Histopathological Whole-Slide Images. *Journal of Pathology Informatics*, *9*(1), 20. https://doi.org/10.4103/jpi.jpi_69_17

[13] Hua, K.-L., Trang, H. T., Srinivasan, K., Chen, Y.-Y., Chen, C.-H., Sharma, V., & Zomaya, A. Y. (2019). Reduction of Artefacts in JPEG-XR Compressed Images. *Sensors*, *19*(5), 1214. https://doi.org/10.3390/s19051214

[14] Iwahashi, M., & Kiy, H. (2013). Non Separable Two Dimensional Discrete Wavelet Transform for Image Signals. In Dr. A. Al-Asmari (Ed.), *Discrete Wavelet Transforms—A Compendium of New Approaches and Recent Applications*. InTech. https://doi.org/10.5772/51199

[15] Landu, R. S. (2022). Image Compression Using AI: Brief Insights into Deep Learning Techniques and AI Frameworks. *International Journal of Engineering, Science, Technology and Innovation (IJESTI)*, *2*(1), 1–6.

[16] Li, C., Li, L., Jiang, H., Weng, K., Geng, Y., Li, L., Ke, Z., Li, Q., Cheng, M., Nie, W., Li, Y., Zhang, B., Liang, Y., Zhou, L., Xu, X., Chu, X., Wei, X., & Wei, X. (2022). *YOLOv6: A Single-Stage Object Detection Framework for Industrial Applications* (arXiv:2209.02976). arXiv. https://doi.org/10.48550/arXiv.2209.02976

[17] Li, C., Lu, G., Feng, D., Wu, H., Zhang, Z., Liu, X., Zhai, G., Lin, W., & Zhang, W. (2024). *MISC: Ultra-low Bitrate Image Semantic Compression Driven by Large Multimodal Model* (arXiv:2402.16749). arXiv. https://doi.org/10.48550/arXiv.2402.16749

[18] Li, F., & Lukin, V. (2023). Providing a Desired Compression Ratio for Better Portable Graphics Encoder of Color Images: Design and Analysis. In A. J. Tallón-Ballesteros & P. Santana-Morales (Eds), *Frontiers in Artificial Intelligence and Applications*. IOS Press. https://doi.org/10.3233/FAIA230063

[19] Lieberman, K., Diffenderfer, J., Godfrey, C., & Kailkhura, B. (2023). *Neural Image Compression: Generalization, Robustness, and Spectral Biases*. 37th Conference on Neural Information Processing Systems (NeurIPS 2023). https://openreview.net/pdf?id=FxRfAIj4s2

[20] Liu, J., Sun, H., & Katto, J. (2023). Learned Image Compression with Mixed Transformer-CNN Architectures. *2023 IEEE/CVF Conference on Computer Vision and Pattern Recognition (CVPR)*, 14388–14397. https://doi.org/10.1109/CVPR52729.2023.01383

[21] Lu, M., Guo, P., Shi, H., Cao, C., & Ma, Z. (2022). Transformer-based Image Compression. *2022 Data Compression Conference (DCC)*, 469–469. https://doi.org/10.1109/DCC52660.2022.00080

[22] Mishra, D., Singh, S. K., & Singh, R. K. (2021). Wavelet-Based Deep Auto Encoder-Decoder (WDAED)-Based Image Compression. *IEEE Transactions on Circuits and Systems for Video Technology*, *31*(4), 1452–1462. https://doi.org/10.1109/TCSVT.2020.3010627

[23] Ponomarenko, N., Jin, L., Ieremeiev, O., Lukin, V., Egiazarian, K., Astola, J., Vozel, B., Chehdi, K., Carli, M., Battisti, F., & Jay Kuo, C.-C. (2015). Image database TID2013: Peculiarities, results and perspectives. *Signal Processing: Image Communication*, *30*, 57–77. https://doi.org/10.1016/j.image.2014.10.009

[24] Pratt, W. K. (2013). *Introduction to Digital Image Processing* (0 edn). CRC Press. https://doi.org/10.1201/b15731

[25] Rasheed, M. H., Salih, O. M., Siddeq, M. M., & Rodrigues, M. A. (2020). Image compression based on 2D Discrete Fourier Transform and matrix minimization algorithm. *Array*, *6*, 100024. https://doi.org/10.1016/j.array.2020.100024

[26] Shihab, H. S. (2023). Image Compression Techniques on-Board Small Satellites. *Iraqi Journal of Science*, 1518–1534. https://doi.org/10.24996/ijs.2023.64.3.40

[27] Tang, Y., Xiang, T., Yang, Y., & Shu, Z. (2020). JPEG-XR-GCP: Promoting JPEG-XR Compression by Gradient-Based Coefficient Prediction. *2020 12th International Conference on Advanced Computational Intelligence (ICACI)*, 51–58. https://doi.org/10.1109/ICACI49185.2020.9177623

[28] Thomas, S., Krishna, A., Govind, S., & Sahu, A. K. (2025). A novel image compression method using wavelet coefficients and Huffman coding. *Journal of Engineering Research*, *13*(1), 361–370. https://doi.org/10.1016/j.jer.2023.08.015

[29] Umbaugh, S. E. (2017). *Digital Image Processing and Analysis with MATLAB and CVIPtools, Third Edition: Applications with MATLAB® and CVIPtools, Third Edition*. CRC Press. https://doi.org/10.1201/9781351228374

[30] Xu, J., Feng Wu, Jie Liang, & Wenjun Zhang. (2010). Directional Lapped Transforms for Image Coding. *IEEE Transactions on Image Processing*, *19*(1), 85–97. https://doi.org/10.1109/TIP.2009.2032344

Prof. Volodymyr Barannik
e-mail: vvbar.off@gmail.com

Doctor of Technical Sciences, professor, Department of Artificial Intelligence and Software, V. N. Karazin Kharkiv National University.
Scientific interests: information security, image processing, information coding.

https://orcid.org/0000-0002-2848-4524

Ph.D. Mykhailo Babenko
e-mail: babenkomahalych@gmail.com

Associate professor, Dniprovsky State Technical University, Kamianske, Ukraine.
Scientific interests: information security.

https://orcid.org/0000-0003-1013-9383

Ph.D. Dmytro Uzlov
e-mail: dmytro.uzlov@karazin.ua

Director of the Educational and Research Institute of Computer Sciences and Artificial Intelligence V.N. Karazin Kharkiv National University Candidate of Technical Sciences.
Scientific interests: data analysis, artificial intelligence, NLP for criminal intelligence, digital forensics knowledge representation, computational criminology, knowledge graphs for crime analysis, semantic web in law enforcement, computer vision

https://orcid.org/0000-0003-3308-424X

Ph.D. Dmitry Barannik
e-mail: d.v.barannik@gmail.com

Lecturer, researcher Department of Communication Systems and Networks, Kruty Heroes Military Institute of Telecommunications and Information Technology.
Scientific interests: systems, technologies of transformation, encoding, defence and information transfer, semantic processing of images.

https://orcid.org/0000-0002-7074-9864

M.Sc. Yevhenii Yelisieiev
e-mail: eliseev70evgeniy@gmail.com

Ph.D. student, Department of Information and Network Engineering, Kharkov National University of Radio Electronics.
Scientific interests: information security, image processing, information coding.

https://orcid.org/0000-0002-0953-4397

M.Sc. Vladyslav Kostromytskyi
e-mail: vladyslavkostromytskyi@gmail.com

PhD student, Department of Information and Network Engineering, Kharkov National University of Radio Electronics.
Scientific interests: image processing, information coding.

https://orcid.org/0009-0001-2082-5080

M.Sc. Valeriy Barannik
e-mail: valera462000@gmail.com

Ph.D. student, Department of Information and Network Engineering, Kharkov National University of Radio Electronics.
Scientific interests: systems, technologies of transformation, encoding, defence and information transfer, semantic processing of images.

https://orcid.org/0000-0003-3516-5553

Ph.D. Oleh Kompaniiets
e-mail: kompaniets_oleg@i.ua

Doctoral candidate of Ivan Kozhedub Kharkiv National Air Force University Kharkiv, Ukraine.
Scientific interest: coding, information technology, image processing, information coding.

https://orcid.org/0000-0001-7472-0869

Ph.D. Nina Petrukha
e-mail: nninna1983@gmail.com

Ph.D. (Economics), associate professor, docent of the Department of Management in Construction, Kyiv National University of Construction and Architecture.
Scientific interests: information security, image processing, information coding.

https://orcid.org/0000-0002-3805-2215

Ph.D. Artem Bychenko
e-mail: bychenko_artem@nuczu.edu.ua

Candidate of Technical Sciences, associate professor, Head of the Department of Unmanned Systems and Robotics, National University of Civil Defense, Cherkasy, Ukraine.
Scientific interests: information security.

https://orcid.org/0000-0003-3788-3268